Electronic Supplementary Material (ESI) for Journal of Materials Chemistry A.

Solar-assisted urea oxidation at silicon photoanodes promoted by an amorphous and optically-adaptive Ni-Mo-O catalytic layer

Joudi Dabboussi,[a] Rawa Abdallah,[b] Lionel Santinacci,[c] Sandrine Zanna,[d] Antoine Vacher,[a]

Vincent Dorcet,[a] Stéphanie Fryars,[a] Didier Floner,[a] Gabriel Loget*[a]

a. Univ Rennes, CNRS, ISCR (Institut des Sciences Chimiques de Rennes)-UMR6226, Rennes F-35000, France. gabriel.loget@univ-rennes1.fr

b. Lebanese University, EDST, AZM Center for Research in Biotechnology and Its Applications Laboratory of Applied Biotechnology, LBA3B, El Mitein Street, Tripoli, Lebanon.

c. Aix-Marseille Univ., CNRS, CINaM, Marseille, France.

d. Chimie ParisTech – CNRS, PSL University, Institut de Recherche de Chimie Paris, Physical Chemistry of Surfaces Group, 11 rue Pierre et Marie Curie, 75005 Paris, France

Table of contents

1- Experimental section

Materials and reagents

Acetone (electronic grade MOS, Erbatron by Carlo Erba reagents), anhydrous ethanol (RSE electronic grade, Erbatron by Carlo Erba reagents) and ultrapure water (resistivity of 18.2 MΩ cm (Purelab Classic UV)) were used without further purification. The chemicals used for the cleaning and etching of the Teflon vials and the Si wafers were sulfuric acid (96%, Very Large Scale Integration (VLSI, grade Selectipur) and hydrogen peroxide (30%, VLSI, Sigma Aldrich) purchased from BASF and Sigma Aldrich, respectively. Electrolysis solutions were made of KOH (≥85%, pellets for analysis) purchased from Merck and urea (CH_4N_2O; ≥99.5%) purchased from Sigma Aldrich. The solution used for the synthesis of catalyst was composed of sodium molybdate ($Na_2MoO_4.2H_2O$, 98%) and nickel nitrate ($Ni(NO_3)_2.6H_2O$, 98%) which were purchased from Sigma Aldrich, the purity of the Ni target is 99.8% (Leica brand (EM ACE600)), epoxy adhesive was purchased from Loctite.

Surface preparation

All Teflon vials and tweezers used for cleaning silicon were previously decontaminated in 3/1 v/v concentrated H_2SO_4/30% H_2O_2 at 105 °C for 30 min, followed by copious rinsing with ultrapure water. *Caution:* the concentrated aqueous H_2SO_4/H_2O_2 (piranha) solution is very dangerous, particularly in contact with organic materials and should be handled extremely carefully. The *n*-type silicon wafers (resistivity 0.3 to 0.7 Ω cm, phosphorus-doped, 475-525 µm, (100)) were purchased from Siltronix and p^{++}-type silicon wafers (resistivity 0.001 to 0.005 Ω cm, boron-doped, single side polished, 490–510 µm, (100)) were purchased from University Wafers. All the Si surfaces were degreased by sonication in acetone, ethanol, and ultrapure water for 10 min, respectively. The Si surfaces were then decontaminated and oxidized in piranha solution at 105 °C for 30 min, followed by rinsing with several amounts of ultrapure water and dried under an Argon flow. The Ni thin films were deposited on the clean *n*-Si/SiO_x surfaces by sputtering with a Leica EM ACE600 coating system (Ni target purity: 99.8%). The Argon pressure for sputtering was 2×10^{-2} mbar, and the current was 100 mA. The thickness of the film (17 nm) was determined *in situ* by a quartz crystal microbalance and *ex situ* by AFM. After deposition, the system was degassed with N_2.

Synthesis of catalytic layer

MNO catalytic films were synthesized by an hydrothermal method. For this, 2 mmol of $Ni(NO_3)_2.6H_2O$ and 2 mmol of $Na_2MoO_4.2H_2O$ were added into 35 ml distilled water and stirred for 15 mins. After forming a clear solution, 30 ml of the mixture was transferred to a 50 ml Teflon container that already contained a clean Si/SiO_x/Ni surface (2×2 cm^2) placed at the bottom. The complete setup was placed in a stainless steel autoclave and maintained at 90 °C for 6 hours in an oven. After cooling to room

temperature, the surface was sonicated in ethanol and distilled water for 5 min to remove aggregates and dried under an Argon flow to obtain the $Si/SiO_x/Ni/MNO$. Finally, these substrates were annealed at 300 ° C for 2 hours (heating ramp = 5 °C min^{-1}) under an argon atmosphere.

Electrode fabrication

The surfaces were then processed to fabricate electrodes. First, the backside of the modified surface was scratched with a diamond glass cutter. An Ohmic contact was established on the backside of the Si surface with a metal wire by applying a droplet of InGa eutectic. A layer of silver paste was then painted to cover the InGa eutectic contact as well as a part of the metal wire. After, the active area was defined on the front side with an epoxy-based resin (Loctite 9460, Henkel) that also covered all the backside of the surface. The electrode was then cured in air at room temperature for 3 h. The exact geometrical value of all electrodes was precisely determined using the ImageJ software prior to the photoelectrochemical experiments.

Surface characterization

The crystalline structure of the layers was determined using a high brilliancy rotating anode (Rigaku, RU-200BH) equipped with a Fox3D Cu 12_INF mirror (Xenocs) and an image plate detector (Rayonix, Mar345). The radiation used was Cu K_α, θ = 1.5418 Å and the beam size was 0.5×0.5 mm^2. The chemical composition was determined by XPS using a VG ESCALAB 250 spectrometer (ThermoFisher Scientific). Survey spectra and high-resolution spectra of the C 1s, O 1s, Ni 2p and Mo 3d core-level regions were collected at a take-off angle of 90° and a pass energy of 100 and 20 eV, respectively, using an Al K_α monochromated X-ray source. Data processing was performed using the CasaXPS analysis software, component peaks defined by BE, full width at half maximum (fwhm) and Gaussian/Lorentzian envelopes. BEs of the component peaks were corrected with reference to the C 1s peak for $–CH_2—CH_2–$ bonds set at 284.6 eV.

Scanning electron microscopy (SEM) was performed using a JSM 7100 F (JEOL). The colorized SEM picture of Figure 1b was made using the Inkscape freeware. Transmision Electron Microscopy (TEM) was performed using a JEM 2100 LaB6 (JEOL) operating at 200KV equipped with a scanning module and an Orius 200D CCD camera (Gatan) for Bright Field (BF) imaging and a US1000 CCD camera for high resolution imaging. Elemental mapping was performed using Aztec software with the help of an energy dispersive scattering (EDS) detector X-MAX^N 80T (Oxford). UV-vis transmission spectra was performed using a Shimadzu UV-3600plus spectrophotometer with an integration sphere attachment ISR-603 using barium sulfate surface ($BaSO_4$, Nacalai Tesque) as reflective surface.

Photoelectrochemical measurements

Cyclic voltammetry (CV), chronoamperometry (CA) and electrochemical impedance spectroscopy (EIS) were performed in a photoelectrochemical cell comprising a quartz window into which were inserted a Si/SiO_x/Ni/MNO working electrode, a reference electrode Hg/HgO (1M KOH) and a carbon counter electrode. The cell was filled with a KOH (measured pH = 13.5) or a KOH + urea solution. The epoxy-sealed Si/SiO_x/Ni/MNO surface was placed in front of the quartz window. The light was supplied by a solar simulator (LS0106, LOT Quantum Design) equipped with an AM 1.5G filter. The power intensity of the light source, where the photoanode was located, was adjusted to 100 mW cm^{-2} using an ILT1400 radiometer (International Light Technologies). The CVs reported in this work were recorded at 100 mV s^{-1}. The potentials versus Hg/HgO were converted into potentials versus reversible hydrogen electrode (RHE) using the following relationship:

$$E_{\mathrm{RHE}} = E_{\mathrm{Hg/HgO}} + 0.098 + 0.059\ \mathrm{pH} \qquad (1)$$

Electrochemical measurements were performed with a Zennium potentiostat (Zahner). The electrochemical impedance spectra (EIS) were recorded at a fixed potential of 1 V vs RHE for both OER and UOR in their corresponding electrolytes. The low frequency impedance response was fitted using an equivalent circuit comprising a resistor in series with a capacitance and a resistor in parallel. IPCE measurements were performed with a CIMPS-QE IPCE 3 workstation (Zahner) comprising a TLS03 tunable light source controlled by a PP211 potentiostat in the same cell as the one used for classical electrochemical experiments. The Thales software provided the spectra in photocurrent efficiency (A W^{-1}) or IPCE (%). In order to check the validity of the IPCE measurements, the IPCE spectrum obtained in UOR condition was first converted into photocurrent density (in A W^{-1}). We then used the AM 1.5G reference solar spectrum obtained from the ASTM (American Society for Testing Materials) webpage (http://rredc.nrel.gov/solar/spectra/am1.5/) in order to extract the incident power distribution as a function of the wavelength in the spectral range of our measurements. Based on these two spectra, the incident power was converted into a photocurrent distribution that was integrated to finally obtain the value of photocurrent densities under AM 1.5G simulated sunlight at 2.1 V. Using these data, an integrated photocurrent density of 20.1 mA cm^{-2} was calculated, in good agreement with what was measured in the voltammetry experiments. The amount of degraded urea after photoelectrolysis was measured using a colorimetric method, inspired by the protocol reported by Knorst *et al.*[1] To do this, a cell with two compartments separated with an anion exchange membrane was filled with 1 M KOH + 50 mM urea. The illuminated working photoelectrode and the reference were immersed in the anodic compartment and the counter electrode (a Ni foam) foam was placed in the cathodic compartment. Electrolysis was done potentiostatically at 1 V vs RHE for 3 h while current was

monitored by CA. After electrolysis, 2 ml of the resulting solution was added to a solution (0.5 ml) containing 4 g of p-dimethylaminobenzaldehyde (Alfa Aesar) in 100 ml of 4% (v:v) sulphuric acid in absolute ethanol, then 0.5 ml of sulphuric acid was added. After 10 min, the absorbance of the solution was measured at 434 nm against a blank cuvette (containing the same solution without urea) using a Jasco V630-BIO spectrophotometer. The concentrations of the yellow-colored compound (attributed to urea) in the samples after electrolysis ($n_{urea,elec}$) was determined using a calibration curve that was done prior to the electrolysis experiment. The charge Q, delivered during the preparative electrolysis, was used to calculate the theoretical value of degraded urea $n_{\text{urea},theo}$ as follows:

$$n_{\text{urea},theo} = \frac{Q}{6F} \quad (2)$$

with F being the Faraday constant. The faradaic efficiency was calculated using the following relationship:

$$\eta = \frac{n_{urea,elec}}{n_{urea,theo}} \times 100 \quad (3)$$

2- Supplementary figures

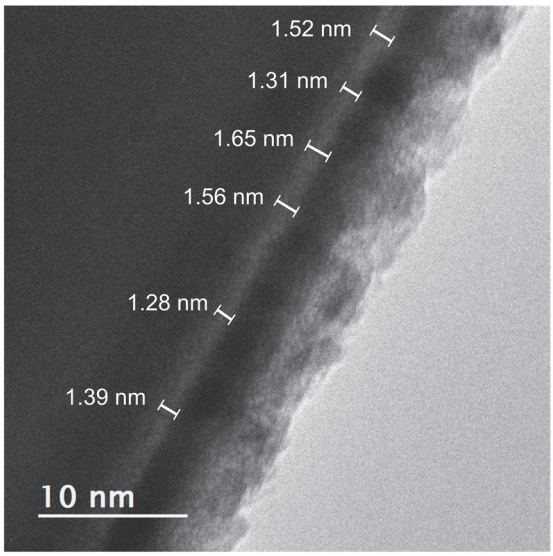

Figure S1. TEM picture showing the *n*-Si/SiO_x/Ni interface. Note that, in this case, the NMO coating and a part of the Ni thin film was etched away by ion milling.

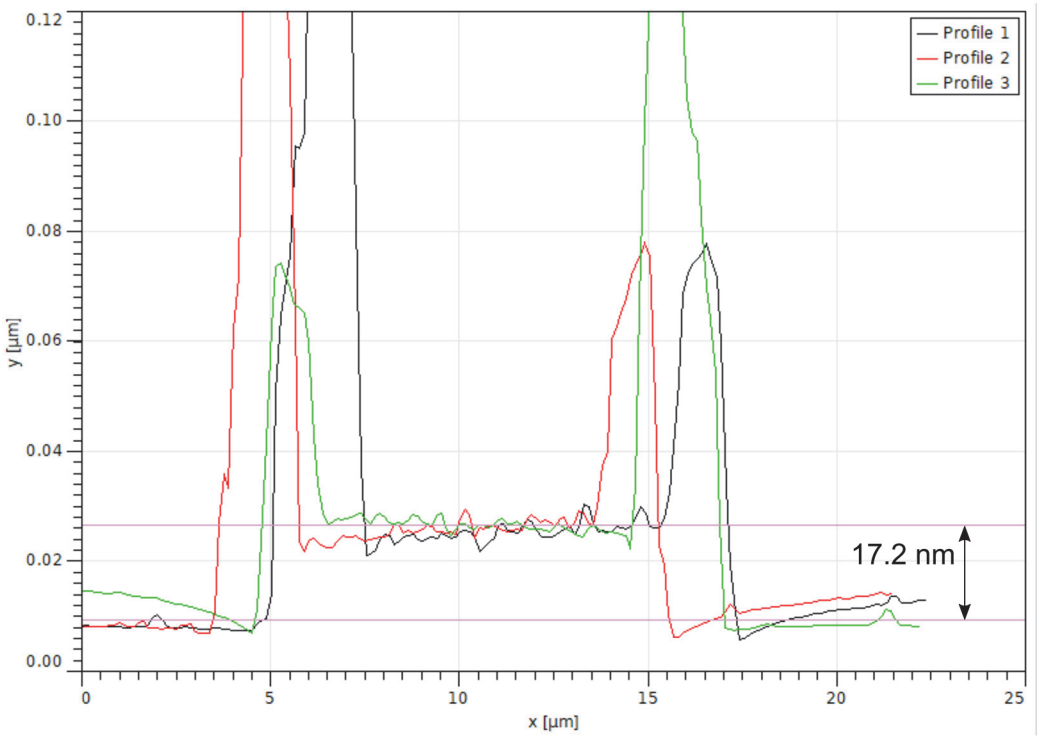

Figure S2. Three AFM profiles, obtained after a lift-off process, showing the thickness of the Ni thin film deposited by sputtering on *n*-Si/SiO_x.

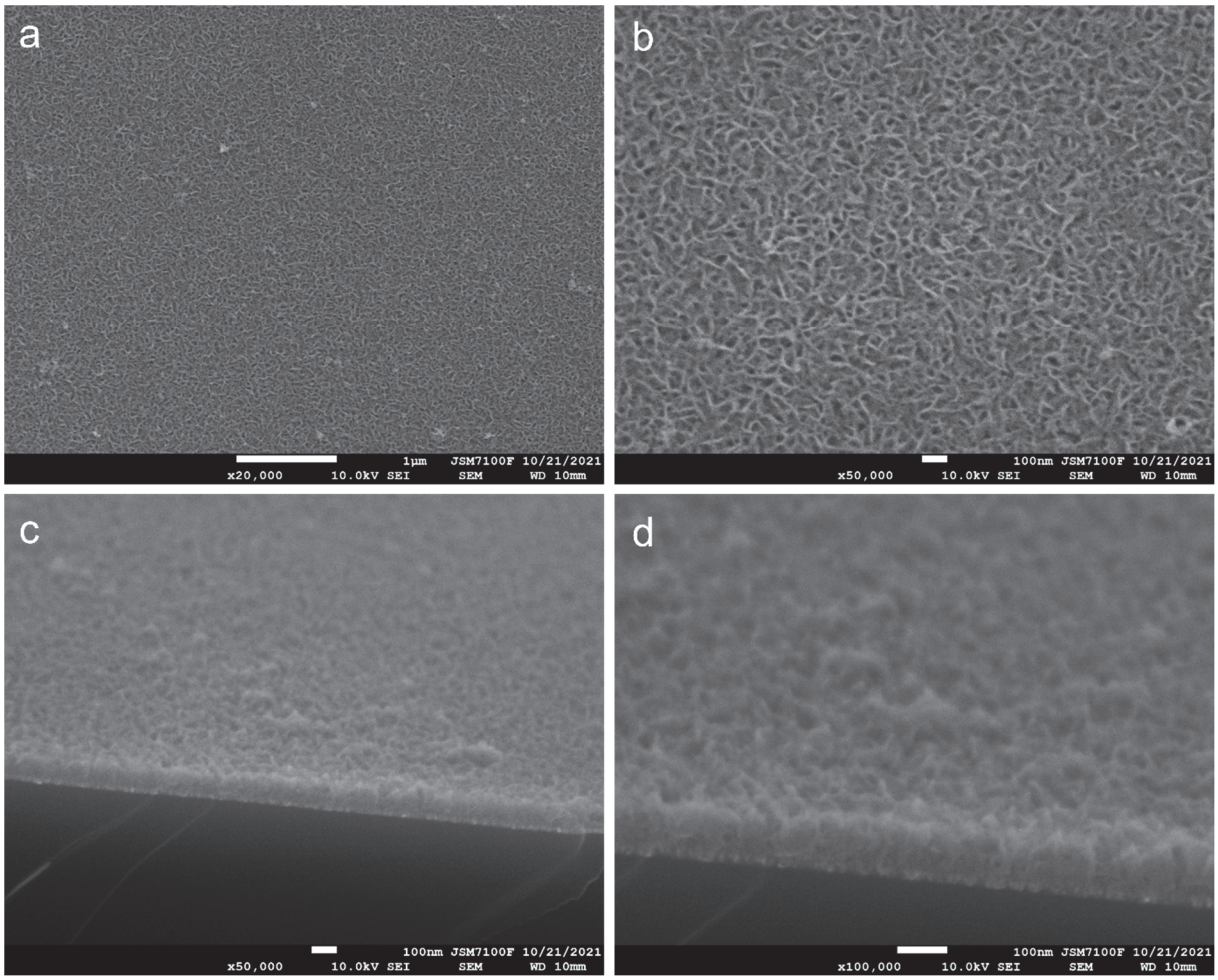

Figure S3. a,b) Top view and c,d) cross-section SEM pictures of a *n*-Si/SiO_x/Ni/NMO surface.

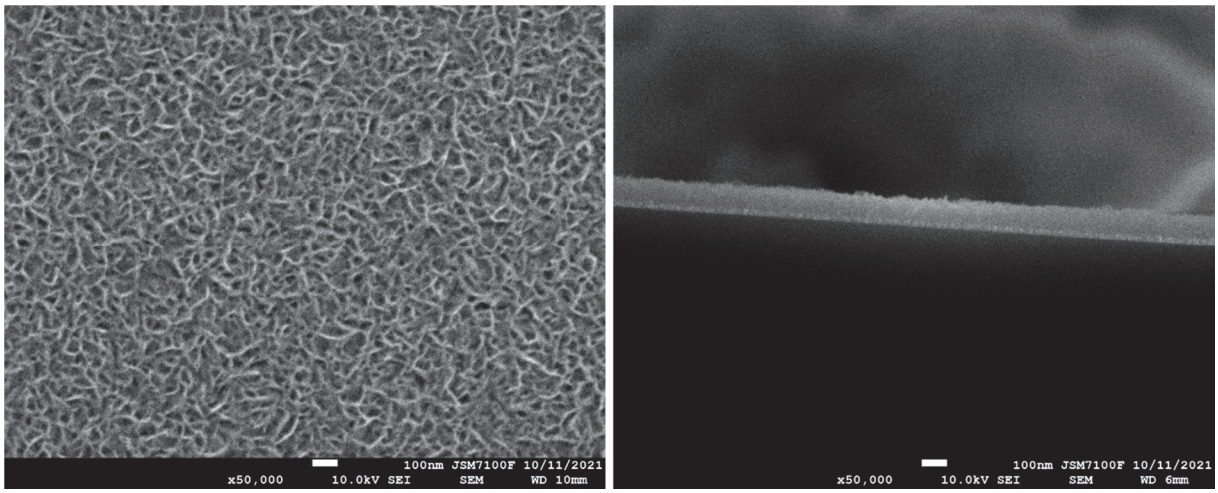

Figure S4. SEM pictures of an *n*-Si/SiO_x/Ni/NMO surface that has not been annealed.

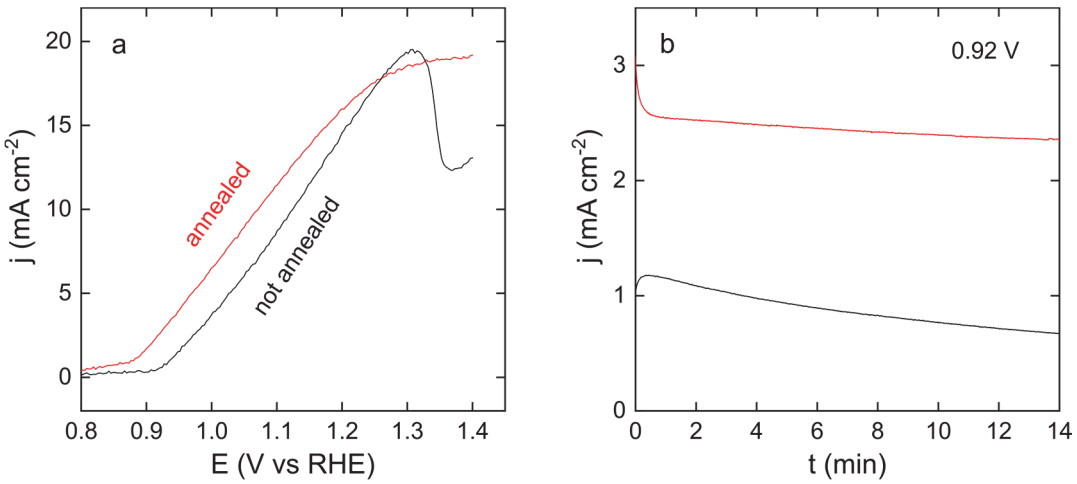

Figure S5. a) Linear sweep voltammograms (scan rate of 100 mV s^{-1}) recorded under illumination on a not-annealed (black curve) and an annealed (red curve) *n*-Si/SiO_x/Ni/NMO photoanode in 1 M KOH + 0.33 M urea. b) CAs recorded under illumination at a potential of 0.92 V with a not annealed (black curve) and an annealed (red curve) *n*-Si/SiO_x/Ni/NMO photoanode in 1 M KOH + 0.33 M urea.

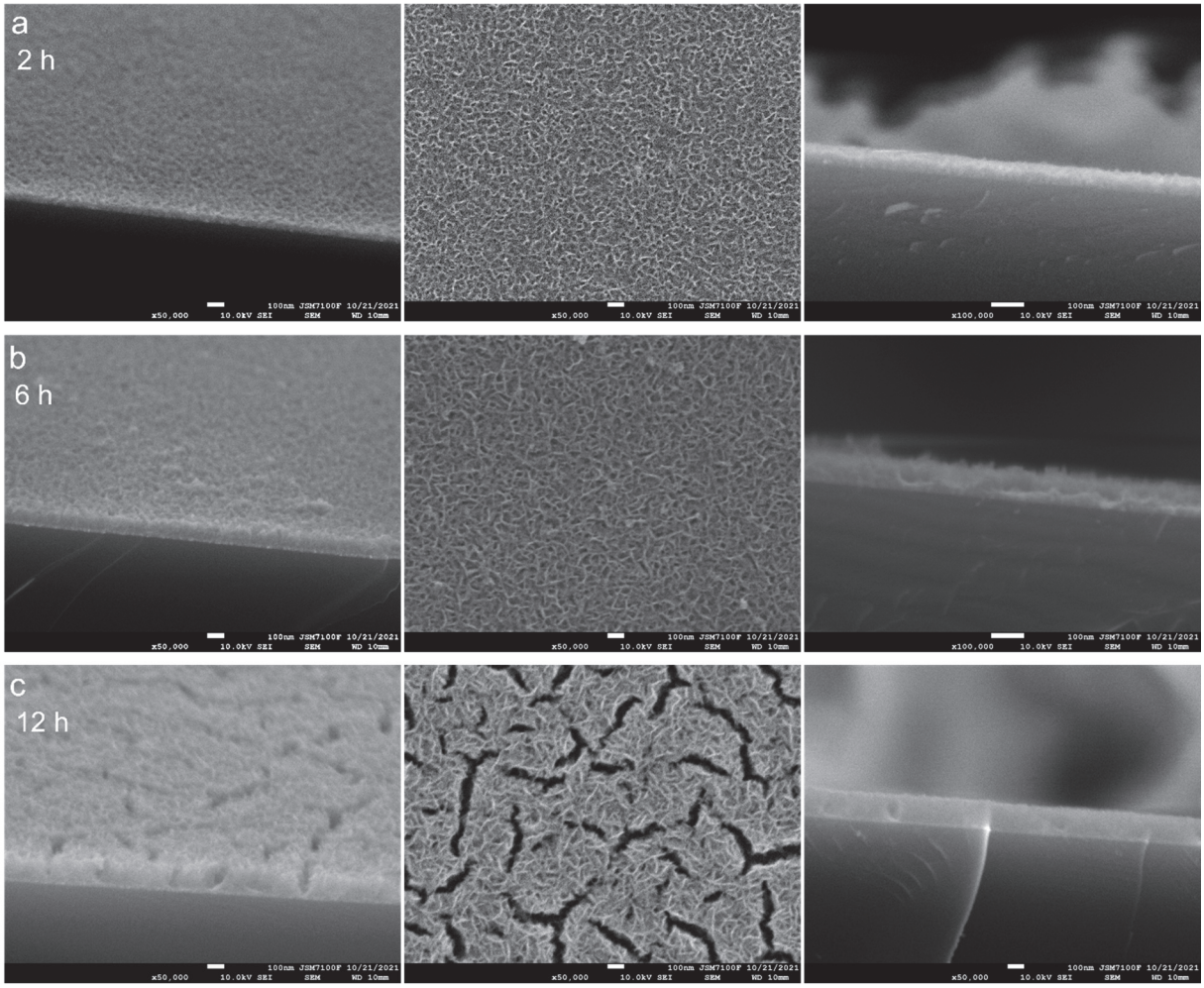

Figure S6. SEM pictures showing *n*-Si/SiO_x/Ni/NMO surfaces obtained with coating times of a) 2 h, b) 6 h, and c) 12 h.

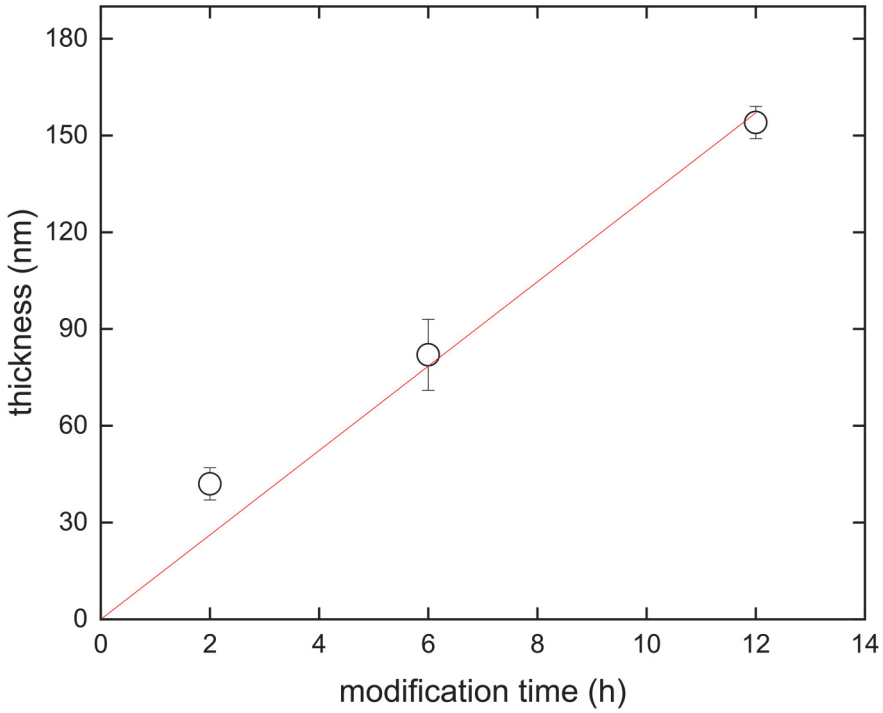

Figure S7. Graph of the NMO coating thickness as a function of the modification time. The thickness of the coating (disks) was determined by measuring the total thickness of the deposit onto Si by SEM and subtracting the thickness of the deposited Ni thin film (17 nm). The red line is a linear fit of the data.

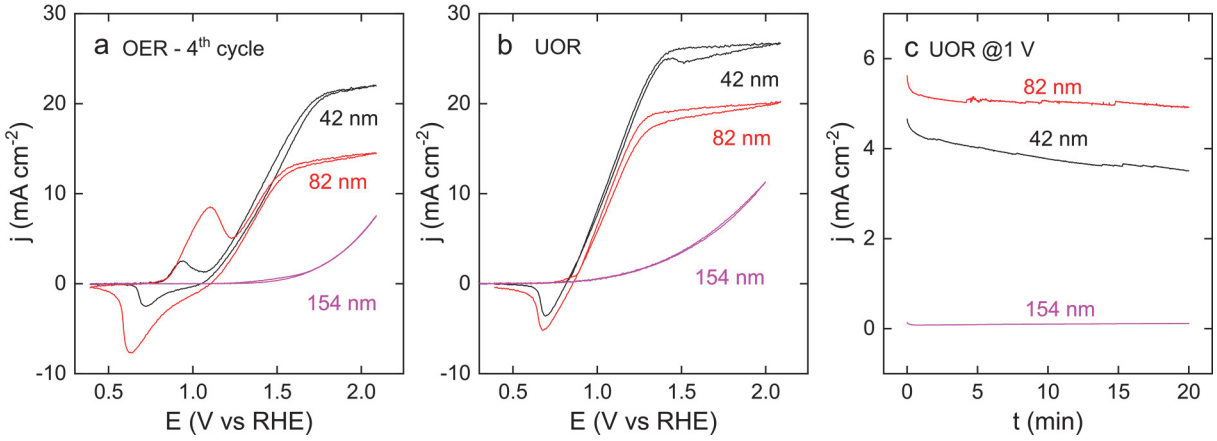

Figure S8. a) CVs (scan rate of 100 mV s^{-1}, 4th cycle) recorded in 1 M KOH under illumination on *n*-Si/SiO_x/Ni modified with NMO layers having thicknesses of 42 (black), 82 (red), and 154 nm (pink). b) CVs recorded in 1 M KOH + 0.33 M urea under illumination on *n*-Si/SiO_x/Ni modified with NMO layers having thicknesses of 42 (black), 82 (red), and 154 nm (pink). c) CAs recorded under illumination in 1 M KOH + 0.33 M urea at a potential of 1 V illumination on *n*-Si/SiO_x/Ni modified with NMO layers having thicknesses of 42 (black), 82 (red), and 154 nm (pink).

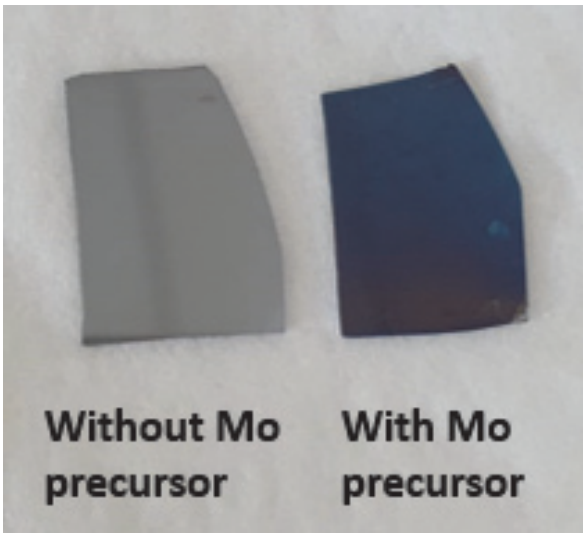

Figure S9. Photograph showing *n*-Si/SiO_x/Ni surfaces after hydrothermal modification without (left) and with (right) 57 mM sodium molybdate. No coating was observed when the Mo precursor was absent.

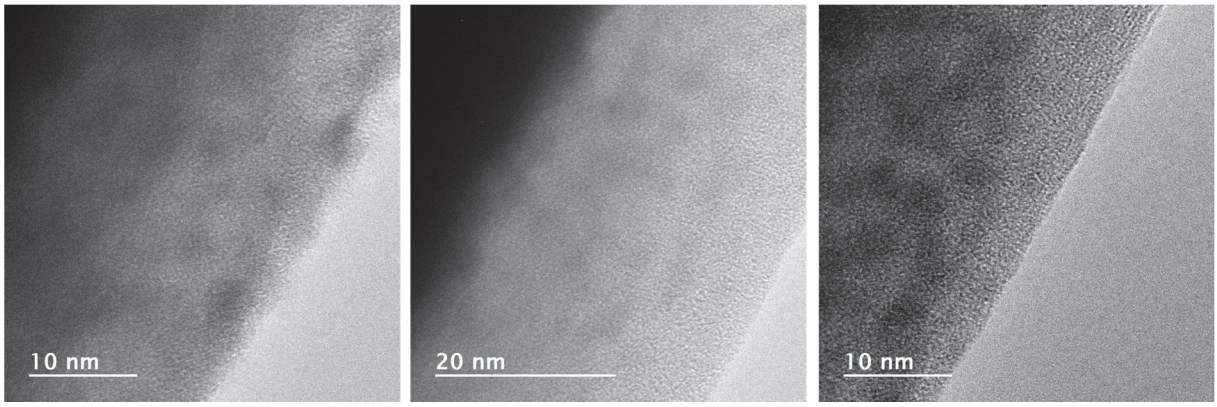

Figure S10. High resolution TEM pictures of the NMO coating.

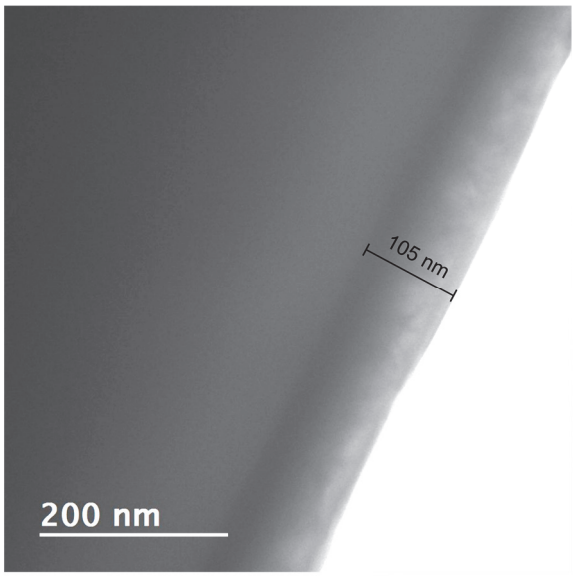

Figure S11. TEM picture of the *n*-Si/SiO_x/Ni/NMO cross section used for the EDS STEM analysis of Figure 2.

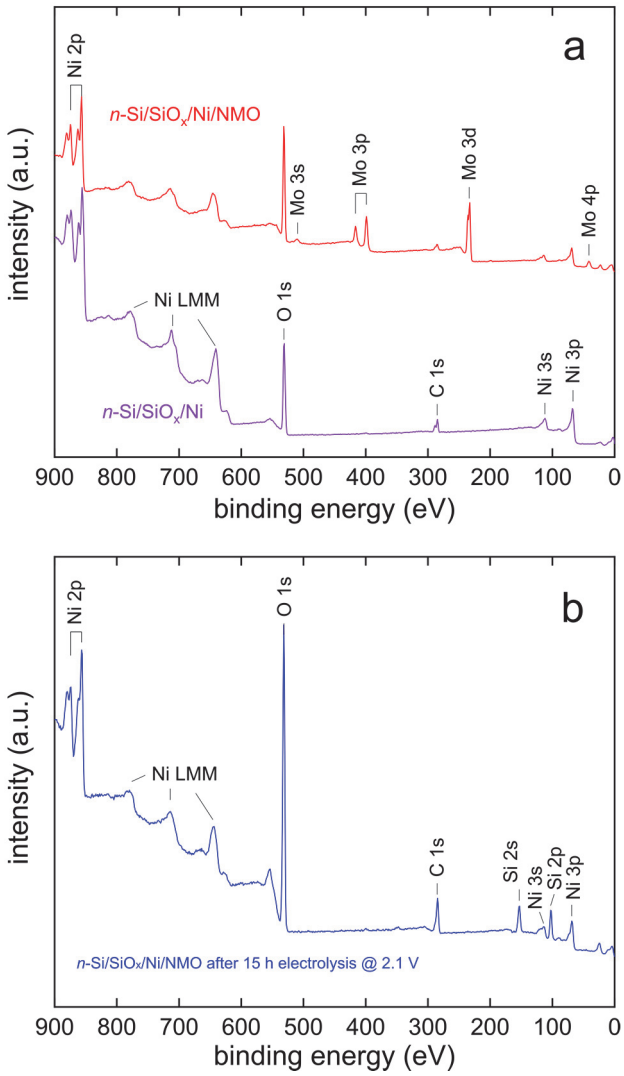

Figure S12. a) XPS survey spectra measured on *n*-Si/SiO_x/Ni (purple) and *n*-Si/SiO_x/Ni/NMO (red). b) XPS survey spectra measured on *n*-Si/SiO_x/Ni/NMO after 15 h of electrolysis at 2.1 V.

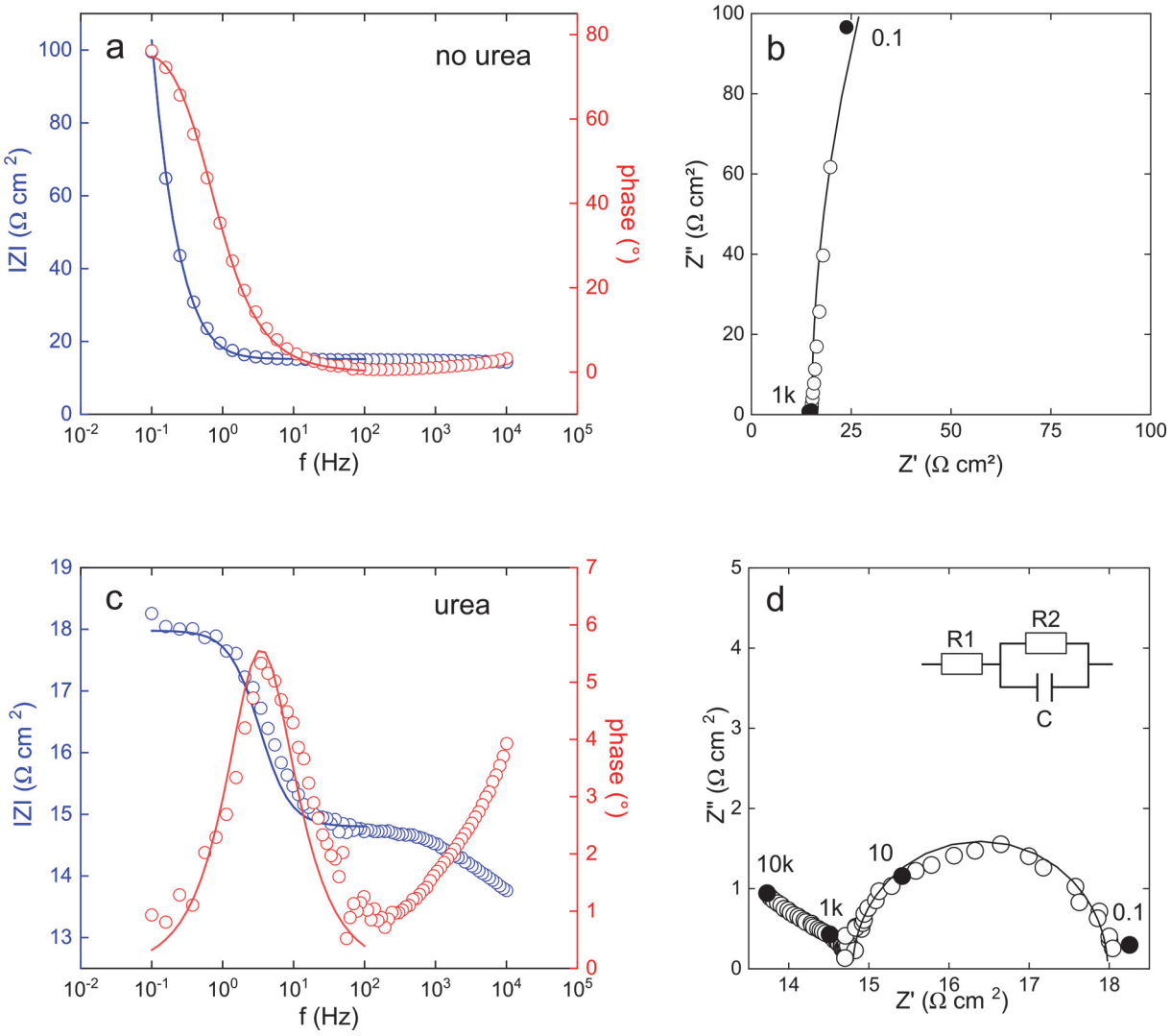

Figure S13. a,c) Bode and b,d) Nyquist representation of the PEIS measurements performed on *n*-Si/SiO_x/Ni/NMO at 1 V under illumination in 1 M KOH, without a,b) and with c,d) 0.33 M urea. Disks are experimental data and lines are fitted data of the 100 to 0.1 Hz region, the equivalent circuit used for data fitting is shown in the inset of d).

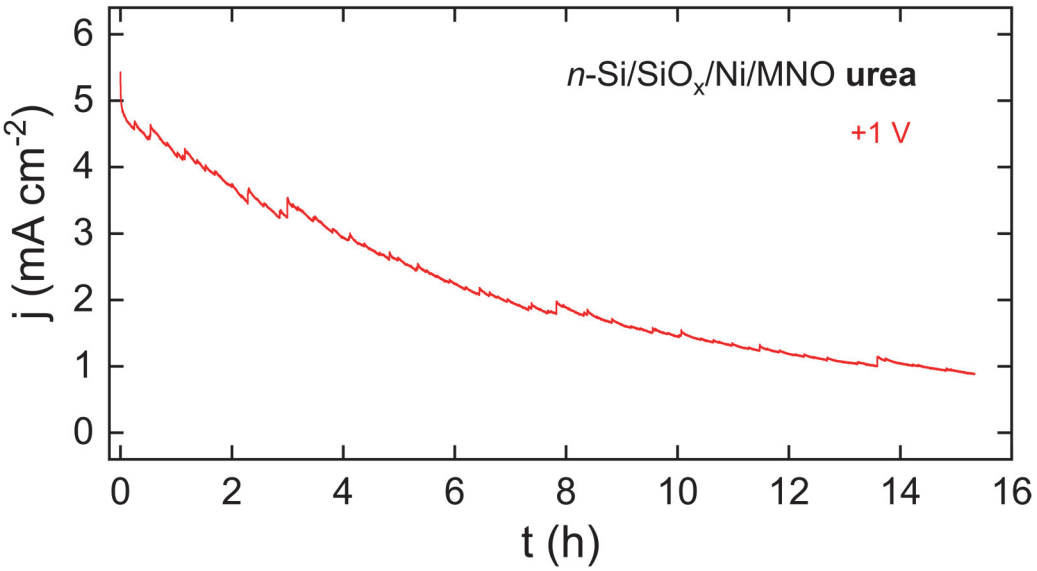

Figure S14. CA recorded under illumination in 1 M KOH with 0.33 M urea on *n*-Si/SiO_x/Ni/NMO at a potential of 1 V.

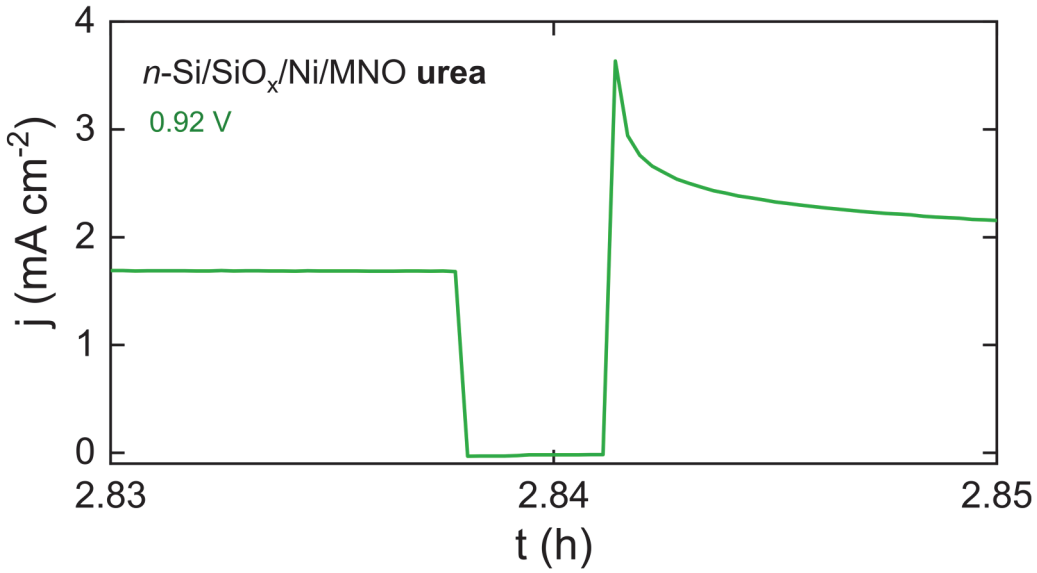

Figure S15. CA showing the interruption of the simulated solar illumination on *n*-Si/SiO_x/Ni/NMO, in 1 M KOH with 0.33 M urea at a potential of 0.92 V.

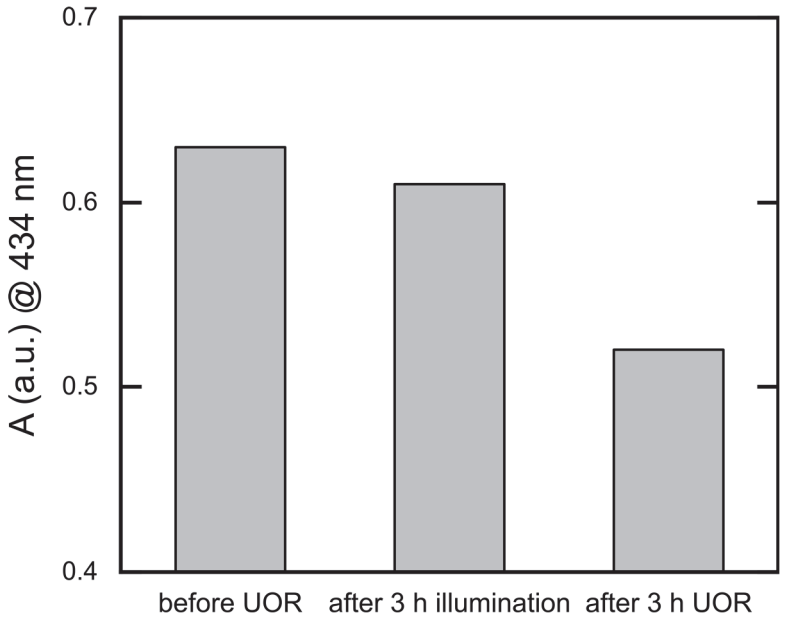

Figure S16. Plot showing the absorbance determined at 434 nm during the colorimetric titration of urea.

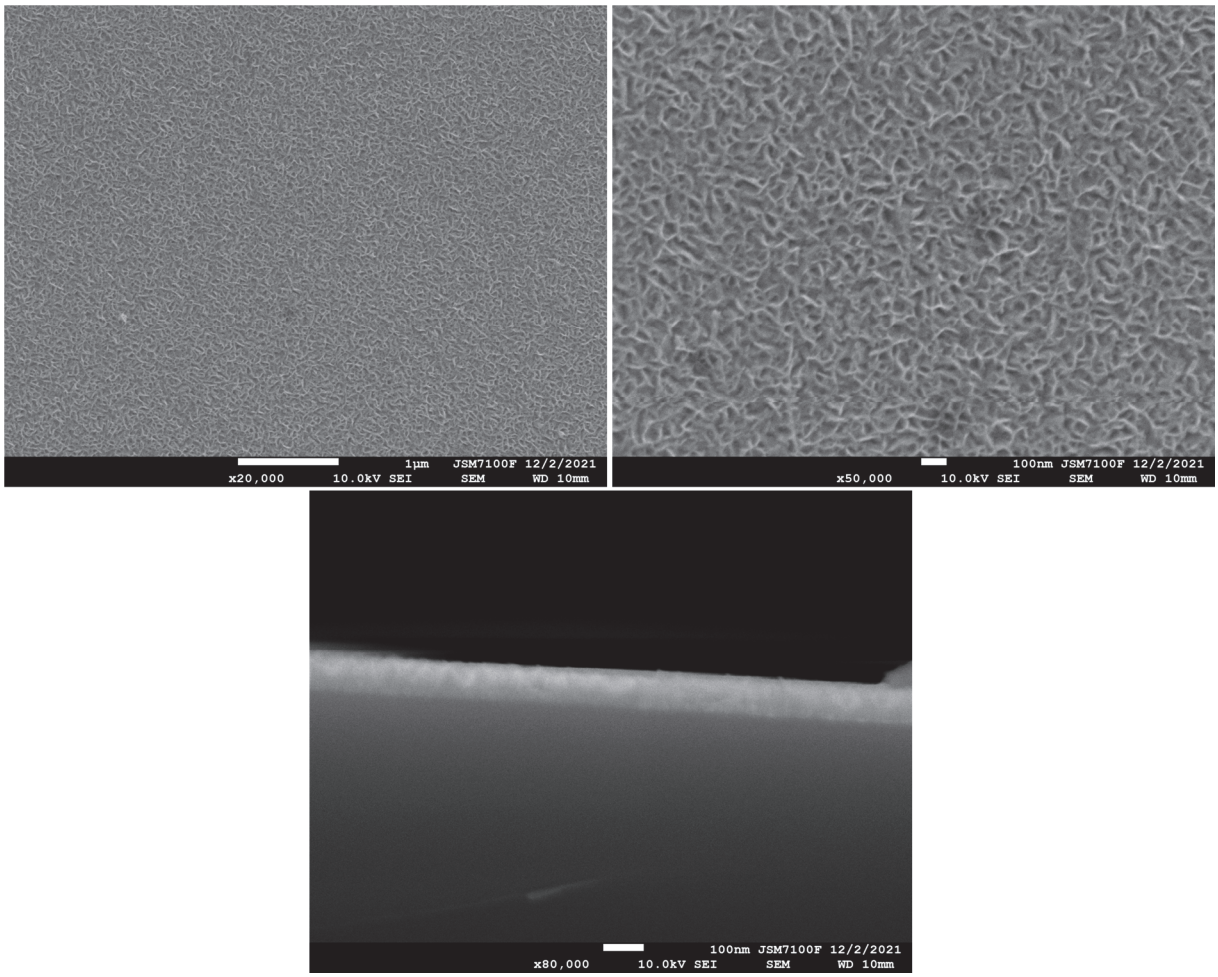

Figure S17. SEM pictures of an *n*-Si/SiO_x/Ni/NMO surface that has been used for 15 h at 2.1 V.

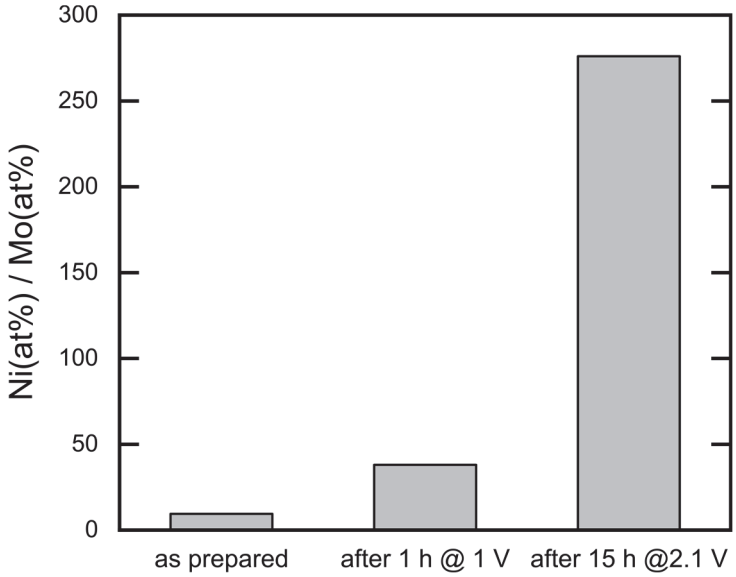

Figure S18. Plot showing the evolution of the ratio between the Ni(at%) and the Mo(at%) determined by EDS on *n*-Si/SiO_x/Ni/NMO.

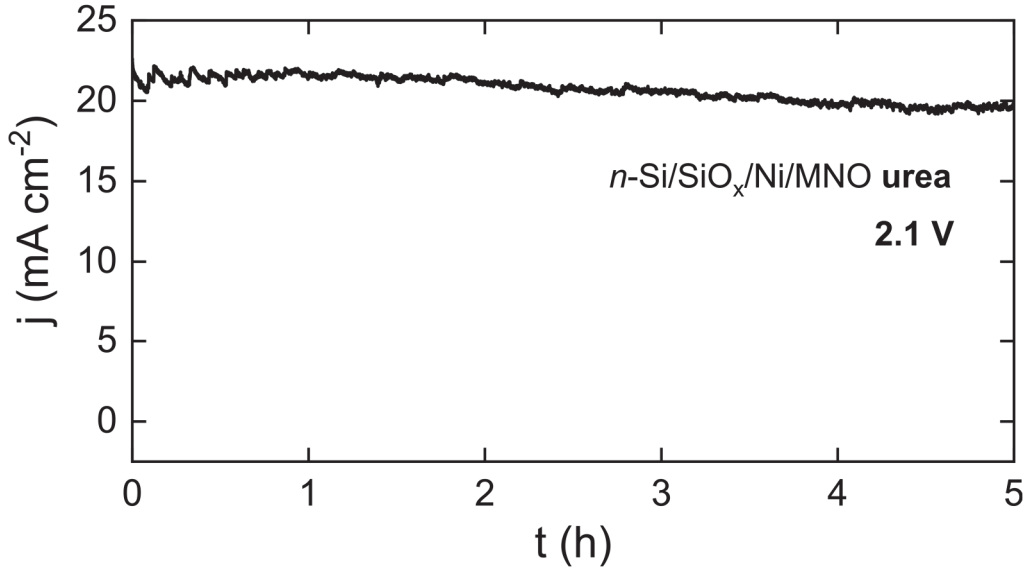

Figure S19. CA recorded under illumination in 1 M KOH with 0.33 M urea on *n*-Si/SiO_x/Ni/NMO at a potential of 2.1 V.

3- Supplementary tables

Table S1. Values of R1, C2 and R2 obtained by fitting the low-frequency PEIS data of Figure S13 (the equivalent circuit is represented in the inset of Figure S13b).

	R1 (Ω)	**C (mF)**	**R2 (Ω)**
no urea	15.2	15.8	850.1
0.33 M urea	14.8	15.8	3.2

Notes on PEIS: *The high frequency part (>100 Hz) of the PEIS data is similar in both cases (with and without urea) and is attributed to processes occurring at the solid/solid interfaces or to the cell and was not fitted. Here, we focused on the low-frequency region (100 Hz > f > 100 mHz) that varied considerably upon addition of urea, which we attribute to processes occurring at the coating/liquid interface. R1 and C are similar in both cases, which is logical because the same photoanode, n-Si/SiO_x/Ni/NMO, is used in both cases, in a similar electrochemical cell. The high areal capacitance of (C = 15.8 mF cm^{-2}) is caused by the rough nature of the NMO deposit and is in the range of that reported for $Ni(OH)_2$/NiOOH coatings.[2] R2, the charge transfer resistance, is much lower in the presence of urea, which confirms the superior photoelectrochemical activity at low overpotential in the presence of urea due to UOR.*

Table S2. Reported operation times for several photoanodes in articles devoted to UOR.

Semiconductor	Layers	Reported operation time (min)	Condition of the stability test	Reference
TiO_2	$Ni(OH)_2$/NiOOH	3000	light limited regime[a]	Energy Environ. Sci. 2012[3]
α-Fe_2O_3	$Ni(OH)_2$/NiOOH	-[b]	-	Energy Environ. Sci. 2012[3]
Ti-doped α-Fe_2O_3	$Ni(OH)_2$/NiOOH	-[b]	-	PCCP 2015[4]
TiO_2/CdS/ZnS	$Ni(OH)_2$/NiOOH	10	-[b]	J. Phys. Chem. C 2018[5]
Co-doped α-Fe_2O_3	Au/ $Ni(OH)_2$/NiOOH	400	0.2 V vs Ag/AgCl[a]	J. App. Electrochem. 2019[6]
SnO_2/$BiVO_4$	$Co_3(PO_4)_2$	60	light limited regime[a]	J. Mater. Chem. A 2019[7]
Si	Ni/$Ni(OH)_2$/NiOOH	10	1.23 V vs RHE[c]	Nat. Commun. 2019[8]
Si	Ni/$Ni(OH)_2$/NiOOH	30	light limited regime[a]	Nat. Commun. 2019[8]
Si	Ni/$Ni(OH)_2$/NiOOH	60	1.23 V vs RHE[d]	J. Phys. Chem. C 2020[9]
Si	Ni/NMO	900	1 V vs RHE[e]	This study
Si	Ni/NMO	300	2.1 V vs RHE[a]	This study

[a]OER may also occur in these conditions. [b]not indicated. [c]according to the CVs in this article, most of the photocurrent originates from UOR. [d]deactivation of the photoelectrode towards UOR occurs rapidly and the remaining photocurrent corresponds likely to OER. [e]only UOR occurs.

4- References

[1] M. T. Knorst, R. Neubert, W. Wohlrab, J. Pharm. Biomed. Anal. 15 (1997) 1627-1632.

[2] A. Pimsawat, A. Tangtrakarn, N. Pimsawat, S. Daengsakul, Sci. Rep. 9 (2019) 16877.

[3] G. Wang, Y. Ling, X. Lu, H. Wang, F. Qian, Y. Tong and Y. Li, Energy Environ. Sci., 2012, 5, 8215–8219.

[4] D. Xu, Z. Fu, D. Wang, Y. Lin, Y. Sun, D. Meng and T. feng Xie, Phys. Chem. Chem. Phys., 2015, 17, 23924–23930.

[5] R. Zhao, G. Schumacher, S. Leahy and E. J. Radich, J. Phys. Chem. C, 2018, 122, 13995–14003.

[6] J. Gan, B. B. Rajeeva, Z. Wu, D. Penley and Y. Zheng, *J. Appl. Electrochem.*, 2020, **50**, 63–69.

[7] J. Liu, J. Li, M. Shao and M. Wei, J. Mater. Chem. A, 2019, 7, 6327–6336.

[8] G. Loget, C. Mériadec, V. Dorcet, B. Fabre, A. Vacher, S. Fryars and S. Ababou-Girard, Nat. Commun., 2019, 10, 3522

[9] P. Aroonratsameruang, P. Pattanasattayavong, V. Dorcet, C. Mériadec, S. Ababou-Girard, S. Fryars and G. Loget, J. Phys. Chem. C, 2020, 124, 25907–25916.